Resonating Valence Bond Wave Function for the Two-Dimensional Fractional Spin Liquid

S. Yunoki and S. Sorella

Istituto Nazionale di Fisica della Materia (INFM)-Democritos, National Simulation Centre, and Scuola Internazionale Superiore di Studi Avanzati (SISSA), I-34014 Trieste, Italy

(Received 13 August 2003; published 15 April 2004)

The unconventional low-lying spin excitations, recently observed in neutron scattering experiments on Cs_2CuCl_4, are explained with a spin liquid wave function. The dispersion relation as well as the wave vector of the incommensurate spin correlations are well reproduced within a projected BCS wave function with gapless and fractionalized spin-1/2 excitations around the nodes of the BCS gap function. The proposed wave function is shown to be very accurate for one-dimensional spin-1/2 systems and remains similarly accurate in the two-dimensional model corresponding to Cs_2CuCl_4, thus representing a good ansatz for describing spin fractionalization in two dimensions.

DOI: 10.1103/PhysRevLett.92.157003 PACS numbers: 74.20.Mn, 71.10.Hf, 75.10.Jm, 71.27.+a

The fractionalization of spin excitations in one-dimensional (1D) spin-1/2 antiferromagnetic (AFM) Heisenberg systems was conjectured by Faddeev and Takhtajan [1] more than 20 years ago, and by now the concept of "spinons," as spin-1/2 elementary excitations for 1D quantum AFM systems, has been well established both theoretically [2] and experimentally [3].

An important and intriguing issue raised by Anderson [4] after the discovery of high-T_C superconductors is whether fractionalized gapless spinons can be defined in even higher dimensions. Many theoretical studies have been done so far analytically [5] and numerically [6], mainly by considering weakly coupled chains. Most studies suggest that unconventional 1D features are very unlikely to occur in higher dimensions since more conventional states, e.g., magnetically ordered, are stabilized with a weak interchain coupling.

The same question can be also addressed experimentally. A series of recent inelastic neutron scattering experiments on Cs_2CuCl_4 by Coldea *et al.* [7,8] showed that, as in 1D systems [3], the spectrum on this material consists of a broad incoherent continuum at each momentum, interpreted as spin fractionalization, despite the fact that the system is clearly two-dimensional (2D). It was also found that the system is described by the following 2D spin-1/2 AFM Heisenberg model (2DAFMHM) on the triangular lattice [see Fig. 1(a)]:

$$H = J\sum_{\langle \mathbf{i},\mathbf{j}\rangle} \vec{S}_{\mathbf{i}} \cdot \vec{S}_{\mathbf{j}} + J' \sum_{\langle\langle \mathbf{i},\mathbf{j}\rangle\rangle} \vec{S}_{\mathbf{i}} \cdot \vec{S}_{\mathbf{j}} \qquad (1)$$

with the intrachain coupling $J = 0.374$ meV and the interchain coupling $J'/J = 0.33$ [7]. Here the symbol $\langle \mathbf{i}, \mathbf{j}\rangle$ ($\langle\langle \mathbf{i}, \mathbf{j}\rangle\rangle$) indicates nearest-neighbor sites along the chain (between different chains). Additional terms such as the Dzyaloshinskii-Moriya interaction and the coupling in the third direction, both of the same order $\simeq$0.02 meV [8], are certainly relevant to explain the various low-temperature phases [7]. However in this study we ignore these much smaller terms as our main purpose is to determine the minimal model and its ground state wave function (w.f.), which may lead to spin fractionalization in the 2D system.

In this Letter we propose a projected BCS w.f. for the ground state of Eq. (1): $|\Phi\rangle = \hat{\mathcal{P}}|\mathrm{BCS}\rangle$, where $|\mathrm{BCS}\rangle$ is the ground state of the following mean-field BCS Hamiltonian:

$$H_{\mathrm{BCS}} = \sum_{\mathbf{k},s} \xi_{\mathbf{k}} c^{\dagger}_{\mathbf{k},s} c_{\mathbf{k},s} + \sum_{\mathbf{k}} [\Delta_{\mathbf{k}} c^{\dagger}_{\mathbf{k},\uparrow} c^{\dagger}_{-\mathbf{k},\downarrow} + \mathrm{H.c.}]. \qquad (2)$$

Here $\xi_{\mathbf{k}} = \epsilon_{\mathbf{k}} - \mu$, $\epsilon_{\mathbf{k}} = -2\cos(\mathbf{k}\cdot\vec{\tau}_1)$, where μ is the chemical potential, $c^{\dagger}_{\mathbf{k},s}$ is the creation operator of an electron with momentum $\mathbf{k}$ and spin $s = \pm 1/2$, and $\Delta_{\mathbf{k}}$ the real gap function for singlet pairing with A_1 symmetry. The variational state $|\Phi\rangle$ for the spin Hamiltonian H is obtained by applying to $|\mathrm{BCS}\rangle$ the

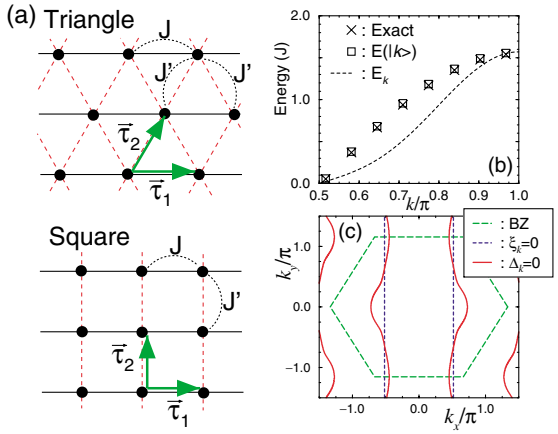

FIG. 1 (color online). (a) Lattice geometries studied. $\vec{\tau}_1$ and $\vec{\tau}_2$ are the primitive translational vectors. (b) Lowest energy spin-1/2 excitations of the 1DAFMHM as a function of momentum $\mathbf{k}$. Dashed line is the BCS spectrum $E_{\mathbf{k}}$ scaled by a factor to match the exact bandwidth. (c) Loci of $\mathbf{k}$ points, where $\xi_{\mathbf{k}} = 0$ (dashed lines) and $\Delta_{\mathbf{k}} = 0$ (solid lines) for $J'/J = 0.33$. The boundary of the first Brillouin zone (BZ) for the triangular lattice is also denoted by long dashed lines.

Gutzwiller projector $\hat{\mathcal{P}}$ onto the subspace of singly occupied sites. The quantities $\Delta_{\mathbf{k}}$ and μ are determined following the variational principle, i.e., by minimizing the energy $E(|\Phi\rangle) = \langle\Phi|H|\Phi\rangle/\langle\Phi|\Phi\rangle$. For this purpose, the Fourier transform $\Delta_{\mathbf{i},\mathbf{j}}$ of $\Delta_{\mathbf{k}}$ is truncated up to the third distance $|\mathbf{i} - \mathbf{j}|$ along the chain so that ten independent parameters for $\Delta_{\mathbf{k}}$ are optimized along with μ [9,10]. In the following, coupled L-site chains for a total number $N = L^2$ of sites with periodic boundary conditions are used unless otherwise stated. In order to explore the quality of $|\Phi\rangle$, the variance of the energy, $\sigma^2(|\Phi\rangle) = \langle\Phi|[H - E(|\Phi\rangle)]^2|\Phi\rangle/\langle\Phi|\Phi\rangle$, is also calculated [11]. For comparison, the same spin liquid w.f. $|\Phi\rangle$ is applied to other models, the uncoupled Heisenberg chains with $J' = 0$ and the 2DAFMHM on the square and the triangular lattices with $J'/J = 0.33$ and $J'/J = 1$, respectively, [see Fig. 1(a)]. For each model the gap function $\Delta_{\mathbf{k}}$ and μ are optimized independently.

The main point of this Letter is that the variational approach represents an accurate theoretical tool for extending the notion of spinons in higher dimensions. With this approach we are able to reproduce the qualitative, as well as the quantitative features of the experiments, confirming the possibility of spin fractionalization in 2D with a transparent theoretical framework. Following Wen [12], we also show that the excitations of H_{BCS} are related to the physical excitations of the spin Hamiltonian.

As a first step, let us verify that the highly nontrivial low-energy spectrum of the 1D spin-1/2 AFM Heisenberg model (1DAFMHM) with nearest-neighbor coupling J is well reproduced by the w.f. $|\Phi\rangle$. It has been well known that $|\Phi\rangle$ describes almost exactly the ground state w.f. [13,14]. Here we show that even the low-lying excited states can be constructed from $|\Phi\rangle$. For the 1D model, the optimized μ is zero, and therefore the BCS spectrum $E_{\mathbf{k}} = \sqrt{\xi_{\mathbf{k}}^2 + \Delta_{\mathbf{k}}^2}$ of Eq. (2) has gapless excitations at $\mathbf{k} = \pm\pi/2$, exactly as the spinon spectrum of the 1DAFMHM does [2]. Since the elementary excitations of H_{BCS} with energy $E_{\mathbf{k}}$ are described by the Bogoliubov modes, $\gamma_{\mathbf{k},s}^{\dagger}$, the simplest variational state for the spinon at momentum $\mathbf{k}$ is $|\mathbf{k}\rangle = \hat{\mathcal{P}}\gamma_{k,\downarrow}^{\dagger}|\mathrm{BCS}\rangle$. To see whether this state $|\mathbf{k}\rangle$ corresponds to a spinon state, we consider a ring with an *odd* number of sites $L = 31$ and a z component of the total spin $S_z^{\mathrm{tot}} = -1/2$. For this case it is known that a well-defined spinon exists only for half of the total Brillouin zone ($\pi/2 \leq |\mathbf{k}| \leq \pi$). As shown in Fig. 1(b), for this branch, the w.f. $|\mathbf{k}\rangle$ represents fairly well the excited state with a spinon at momentum $\mathbf{k}$, as can be verified by the good accuracy in energy. Notice that, although the projection $\hat{\mathcal{P}}$ is crucial to gain a quantitative agreement for the spectrum, the BCS spectrum $E_{\mathbf{k}}$ already gives a qualitatively correct feature of gapless excitations with finite spinon velocity at the right momentum $\mathbf{k} = \pi/2$ [see Fig. 1(b)]. It is also possible to obtain an accurate description for the remaining branch of the spectrum by using a similar variational w.f. with three Bogoliubov modes.

Even in 2D, the elementary excitations of H_{BCS} define quite naturally, after Gutzwiller projection, the spin-1/2 fractionalized excitations of the 2DAFMHM [12]. In order to consider the possibility of spin fractionalization in 2D, it is therefore important to show that the w.f. $|\Phi\rangle$ can appropriately describe the ground state of Eq. (1). The most important effect of frustration on the proposed w.f. $|\Phi\rangle$ is generally to change μ to a nonzero value. This should be contrasted to the case of the 2DAFMHM on the square lattice with no frustration such as the one shown in Fig. 1(a), where the optimized μ is always zero. The reason why $\mu = 0$ in the square lattice for any J'/J is easily explained. For $\mu \neq 0$, H_{BCS} does not possess particle-hole symmetry, and therefore $|\Phi\rangle$ violates the Marshall sign rule [15], which is exact in the square lattice case. Instead, the Marshall sign rule can be violated for $J'/J > 0$ on the triangular lattice, and the gapless excitations of H_{BCS} are no longer located at commensurate points. For example, the optimized value for $N = 18 \times 18$ is $\mu = 0.110(4)$. Thus one can make a spin-1 gapless excitation at wave vector $Q_x = 2\cos^{-1}(-\mu/2) \sim 1.035(2)\pi$, which is close to the experimentally observed incommensurate wave vector on Cs_2CuCl_4 [7]. Indeed, as shown in Fig. 1(c), the nodal lines of $\Delta_{\mathbf{k}}$ intersect the lines defined by $\xi_{\mathbf{k}} = 0$, and thus four gapless modes exist.

To check the quality of the proposed w.f. $|\Phi\rangle$, the variance $\sigma^2(|\Phi\rangle)$ is calculated in Fig. 2(a), where for comparison the variances are also presented for uncoupled chains with $J' = 0$ (spin liquid) and for the 2DAFMHM on the square lattice with $J'/J = 0.33$ (nonspin liquid). As seen in Fig. 2(a), the variance for the triangular case is much smaller than the variance corresponding to the square lattice and instead this value is much closer to the one for the uncoupled chains. To further explore the quality of the w.f., we also calculate in Fig. 2(b) the error of the variational energy from the

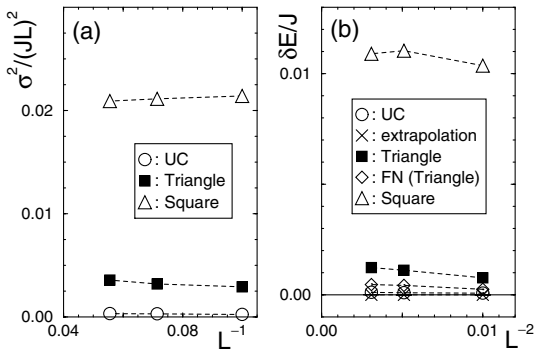

FIG. 2. (a) Variance of energy $\sigma^2(|\Phi\rangle)$ for $N = L \times L$ clusters. UC stands for uncoupled chains. (b) Estimate of the variational error in the energy per site. The FN variational error for the anisotropic triangular lattice and the variance extrapolated error for uncoupled chains are also plotted.

exact value e_0: $\delta E = E(|\Phi\rangle)/N - e_0$. Since the exact energy for the triangular lattice case is not known, we estimate e_0 by extrapolating to zero variance the variational energies corresponding to $|\Phi\rangle$ and to the one Lanczos step w.f. $|\Phi_{1LS}\rangle = (1 + \alpha H)|\Phi\rangle$ with optimized α [9]. Indeed this procedure works well for the uncoupled chains as shown in Fig. 2(b). Though the w.f. $|\Phi\rangle$ for the triangular lattice is not as accurate as for the uncoupled chains, it remains of high quality, much better than the square lattice case. It should also be emphasized that the corresponding values for the best available variational w.f. with explicit AFM order of the widely studied isotropic 2DAFMHM on the square lattice with $J' = J$ [16] are $\sigma^2 \sim 0.015$ and $\delta E \sim 0.004$ in the same unit as in Fig. 2. Also comparing these values to ours, the quality of the w.f. $|\Phi\rangle$ for H is exceptionally good for 2DAFMHM's.

Though the variational approach can provide accurate upper bounds for the energy, it may suffer the well-known difficulty that the low-energy modes are usually insensitive to the total energy, and sometimes completely different w.f.'s give more or less the same energy [17]. In order to reduce this difficulty, quantum Monte Carlo methods, such as a recently developed fixed node (FN) technique, may be used [9,18]. Within this more powerful FN approach, the variational w.f. $|\Phi\rangle$ is used to approximate only the signs of the ground state w.f. In the basis of electron configuration $|x\rangle$, all the off-diagonal matrix elements of the Hamiltonian such that $s_{x'x} = \Phi(x') \times \langle x'|H|x\rangle\Phi(x) < 0$ are considered exact. Instead, all the ones with $s_{x'x} > 0$ are treated semiclassically and traced to the diagonal term, defining an effective FN Hamiltonian H_{FN}. Since the semiclassical approximation is usually good at low energy, we believe that this approach provides a sensible test to examine the stability of the variational w.f. at low energy. Indeed, if, for a properly chosen w.f., $s_{x'x}$ is always nonpositive for $x \neq x'$, then the FN approximation is exact and may change completely the low-energy properties of the variational w.f. Namely, for the 2DAFMHM on the square lattice, it is possible to obtain the exact AFM ordered state provided that the variational w.f. satisfies the Marshall sign rule, a condition that does not necessarily imply AFM order. In the frustrated case no w.f.'s which fulfill $s_{x'x} < 0$ for $x \neq x'$ are known. Therefore, in order to verify the quality of the FN approximation, we estimate by quantum Monte Carlo method the fraction w between the positive and the negative off-diagonal elements. It is found that, due to the quality of our w.f., the ratio w remains very small ($\sim$0.03), implying that H_{FN} contains a large fraction ($\simeq 1 - w$) of matrix elements equal to the exact ones, showing that, in the present case, H_{FN} represents a reliable approximation of H. We finally remark that the ground state $|\Psi_0\rangle$ of H_{FN} can be used as a variational state of H with lower energy [18], $E(|\Psi_0\rangle) \leq E(|\Phi\rangle)$, as clearly seen in Fig. 2(b).

In Fig. 3, the spin correlation functions (z component) $\langle\psi|S_z(\mathbf{i})S_z(\mathbf{j})|\psi\rangle/\langle\psi|\psi\rangle$ are calculated for the

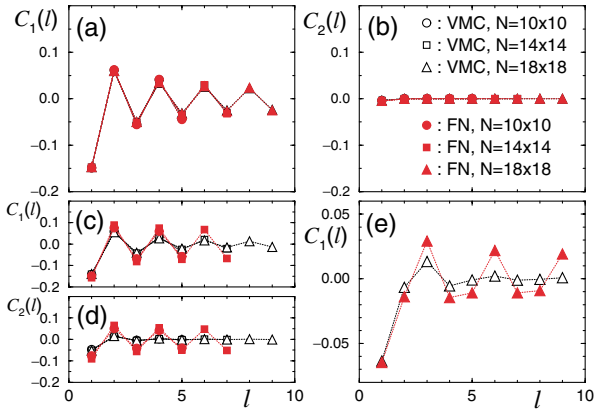

FIG. 3 (color online). Spin correlation functions $C_i(l) = \langle S_z(\vec{r})S_z(\vec{r} + l\vec{\tau}_i)\rangle$ as a function of distance l along the $\vec{\tau}_i$ directions (see Fig. 1) for the 2DAFMHM on the triangular lattice with $J'/J = 0.33$ (a),(b) and $J'/J = 1.0$ (e), and on the square lattice with $J'/J = 0.33$ (c),(d). Open and solid marks are for the variational (VMC) and FN calculations, respectively. Lines are guides to the eye.

2DAFMHM on both the triangular and square lattices using the variational ($|\psi\rangle = |\Phi\rangle$) and the FN ($|\psi\rangle = |\Psi_0\rangle$) methods. For the square geometry, it is clear that the FN approach considerably enhances the large distance correlations, suggesting that the spin liquid state is unstable toward AFM long-range order, in agreement with previous studies [6]. A completely different scenario is evident for the triangular geometry where these long distance correlations do not appreciably change with respect to the variational $|\Phi\rangle$, strongly indicating that the spin liquid state $|\Phi\rangle$ is stable, namely, close to the exact ground state, at least for the clusters studied.

In order to show further the reliability of our calculations, the spin correlation functions for the isotropic 2DAFMHM on the triangular lattice with $J' = J$ are also calculated in Fig. 3(e). Here a $\hat{\mathcal{P}}|\mathrm{BCS}\rangle$ with good variational energy is obtained with $\xi_{\mathbf{k}} = 0$ and a simple gap function with $\Delta_{\mathbf{i},\mathbf{j}} = \pm 1$ restricted up to second nearest distances and with properly chosen signs [19]. Notice that, even by using such a simple spin liquid w.f. with a rather large value of $w \sim 22\%$, the FN method correctly reproduces the classical three sublattice antiferromagnetic correlations [20].

Encouraged by the above results, we now consider the low-lying excitations on the spin liquid state $|\Phi\rangle$ for the 2DAFMHM on the triangular lattice with $J'/J = 0.33$. To this end the FN method is applied. Since w is rather small for this case, we expect that this approach should give a reliable description of the exact excitation spectrum of H. By using the forward walking technique [21], one can evaluate the imaginary time (τ) evolution of the following quantity:

$$S(\mathbf{k}, \tau) = \frac{\langle\Phi|S_z(\mathbf{k})e^{-\tau H_{\mathrm{FN}}}S_z(-\mathbf{k})|\Psi_0\rangle}{\langle\Phi|e^{-\tau H_{\mathrm{FN}}}|\Psi_0\rangle}, \qquad (3)$$

where $S_z(\mathbf{k}) = \sum_{\mathbf{r}} e^{i\mathbf{k}\cdot\mathbf{r}}S_z(\mathbf{r})/\sqrt{N}$. By simple inspection,

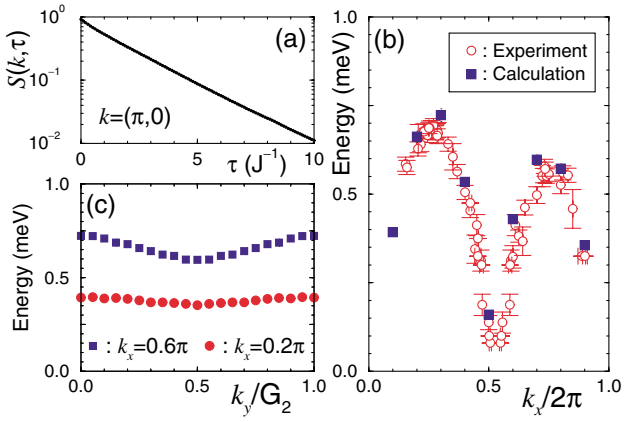

FIG. 4 (color online). (a) A typical semilog plot of the imaginary time correlation function. (b) Calculated spin-1 excitation energies (solid squares) along $\mathbf{k}//\vec{\tau}_1$ for the anisotropic triangular lattice with $N = 10 \times 20$, $J'/J = 0.33$, and $J = 0.374$ meV. (c) The same as in (b) but along $\mathbf{k} \perp \vec{\tau}_1$ for different k_x. Here $G_2 = 4\pi/\sqrt{3}$. For comparison, experimental data on Cs_2CuCl_4 [8] (open circles) are also shown in (b).

the lowest spin-1 excitation energy $E_{\mathbf{k}}^{S=1}$ of H_{FN} can be obtained by fitting the large τ behavior of $S(\mathbf{k}, \tau) \propto e^{-E_{\mathbf{k}}^{S=1}\tau}$. An example of how the method works is given in Fig. 4(a). For large τ, $\ln S(\mathbf{k}, \tau)$ is almost linear and thus we can estimate the lowest excitation energy for each $\mathbf{k}$. The results are summarized in Figs. 4(b) and 4(c). While the spectrum has a strong 1D characteristic, it shows a visible and nontrivial dispersion in the $\mathbf{k}$ direction perpendicular to $\vec{\tau}_1$. Moreover, as seen in Fig. 4(a), the linear fit is not perfect in the intermediate times $\tau J \simeq 1$, implying that there are higher energy ($\sim J$) contributions to the spectrum, suggesting that the full spectrum of the dynamical structure factor may be consistent with the incoherent continuum observed in the experiments. The extremely good agreement between the calculated spectrum and the available experimental data [7], shown in Fig. 4(b), indicates that the 2D model of Eq. (1) describes correctly the experiments, thus supporting the appearance of a spin liquid state. Since no sizable magnetic order was found in this 2D model (Fig. 3), it is very likely that the experimentally observed ordered phases at very low temperatures should be due to only 3D effects [8]. We cannot exclude the possibility that a small spin gap could remain in the thermodynamic limit, as our numerical resolution is limited in the available finite size clusters.

In conclusion, we have shown that, by studying several models, a simple variational approach is capable of describing the ground state properties as well as the low-lying excitations of a spin liquid not only for 1D systems but also for a 2D frustrated spin-1/2 model. Within this approach, it appears that, when the H_{BCS} spectrum remains gapless at commensurate $\mathbf{k}$ as in a nonfrustrated square lattice, the spin fractionalized state undergoes a magnetic instability. By contrast, in the frustrated triangular case, the H_{BCS} spectrum becomes gapless at incommensurate $\mathbf{k}$ as soon as $J'/J > 0$, and it appears much more difficult to destabilize the fractionalized state by a magnetic phase transition. It should be emphasized that both the experimental and the present numerical work consistently suggest that a spin liquid with gapless spin-1/2 excitations appears possible in 2D, its stability being intimately related to the incommensurate momenta of the gapless modes.

Our results may have some impact even for high-T_C superconductors, where the carrier doping naturally leads to incommensurate nodal Fermi points. The existence of a nodal spin liquid has been also conjectured before for interacting Bose systems [22,23], where a Bose metal is the natural bosonic counterpart of a spin liquid with gapless spin excitations and no magnetic order.

We acknowledge R. Coldea for sending us the experimental data and F. Becca and L. Arrachea for providing us the exact diagonalization data. This work is supported by INFM-MALODI and MIUR-COFIN 2003.

[1] L. D. Faddeev and L. A. Takhtajan, Phys. Lett. A **85**, 375 (1981).
[2] See, e.g., *Exactly solvable models of strongly correlated electrons*, edited by V. E. Korepin and H. L. Essler (World Scientific, Singapore, 1994).
[3] D. A. Tennant *et al.*, Phys. Rev. Lett. **70**, 4003 (1993).
[4] P.W. Anderson *et al.*, Phys. Rev. Lett. **58**, 2790 (1987).
[5] S. P. Strong and A. J. Millis, Phys. Rev. Lett. **69**, 2419 (1992); Phys. Rev. B **50**, 9911 (1994); M. Fabrizio *et al.*, Phys. Rev. B **46**, 3159 (1992); C. Castellani *et al.*, Phys. Rev. Lett. **72**, 316 (1994); H. J. Schulz, Phys. Rev. B **53**, 2959 (1996); P. Kopietz *et al.*, Phys. Rev. B **56**, 7232 (1997); Z. Weihong *et al.*, Phys. Rev. B **59**, 14367 (1999).
[6] A.W. Sandvik, Phys. Rev. Lett. **83**, 3069 (1999).
[7] R. Coldea *et al.*, Phys. Rev. Lett. **86**, 1335 (2001); Phys. Rev. Lett. **88**, 137203 (2002).
[8] R. Coldea *et al.*, Phys. Rev. B **68**, 134424 (2003).
[9] S. Sorella, Phys. Rev. B **64**, 024512 (2001); cond-mat/0201388
[10] The nearest-neighbor hoppings along $\vec{\tau}_2$ and $\vec{\tau}_2 - \vec{\tau}_1$ were also optimized and found to be negligibly small.
[11] Only when $|\Phi\rangle$ is an exact eigenstate $\sigma^2(|\Phi\rangle) = 0$, and the smaller is its value, the better is the quality of $|\Phi\rangle$.
[12] X. G. Wen, Phys. Rev. B **44**, 2664 (1991).
[13] S. Sorella *et al.*, Phys. Rev. Lett. **88**, 117002 (2002).
[14] C. Gros, Ann. Phys. (N.Y.), **189**, 53 (1989).
[15] W. Marshall, Proc. R. Soc. London A **232**, 48 (1955).
[16] See, e.g., A. Himeda and M. Ogata, Phys. Rev. B **60**, R9935 (1999).
[17] S. Liang *et al.*, Phys. Rev. Lett. **61**, 365 (1988).
[18] D. F. B. ten Haaf *et al.*, Phys. Rev. B **51**, 13039 (1995).
[19] P. Fendley *et al.*, Phys. Rev. B **66**, 214513 (2002).
[20] See, e.g., B. Bernu *et al.*, Phys. Rev. B **50**, 10048 (1994).
[21] M. Calandra and S. Sorella, Phys. Rev. B **57**, 11446 (1998).
[22] D. Das and S. Doniach, Phys. Rev. B **60**, 1261 (1999).
[23] A. Paramekanti *et al.*, Phys. Rev. B **66**, 054526 (2002).